Progress In Electromagnetics Research Letters, Vol. 43, 175–184, 2013

MICROSTRIP WIDEBAND BANDPASS FILTER BASED ON SQUARE RING LOADED RESONATOR

Kun Deng*, Jian-Zhong Chen, Shou-Jia Sun, Bian Wu, and Chang-Hong Liang

National Laboratory of Science and Technology on Antennas and Microwaves, Xidian University, Xi'an, Shaanxi 710071, P. R. China

Abstract—In this paper, a compact microstrip wideband bandpass filter (BPF) based on square ring loaded resonator (SRLR) is proposed. The SRLR is formed by loading a pair of bent open-stubs outside the diagonal corners of a square ring, which generates three split degenerated modes. The first two split modes form a dominant wideband passband. By introducing another pair of loaded open-stubs, the third split mode is moved into the passband to achieve an extra bandwidth for the wideband passband. Measured results show that this proposed BPF has a 3 dB fractional bandwidth of 69%, and the insertion loss of the BPF is less than 1.0 dB.

1. INTRODUCTION

Wideband bandpass filters (BPFs) with high performance and low cost are extremely desirable in RF/microwave systems. In recent years, different resonators such as multi-mode resonator (MMR) [1, 2], parallel-coupled three lines [3], ring resonator [4, 5], substrate integrated waveguide (SIW) [6] and stub loaded resonator [7] have been proposed to design wideband bandpass filters. In all these structures, ring resonator filters can provide a small circuit size and thus being attractive for designer. A square ring loaded resonator (SRLR) with loaded open stubs was described for wideband BPF operation in [8], which achieves a smaller circuit size than conventional ring resonator wideband BPFs [9–14].

In this paper, a wideband BPF based on a SRLR and loaded stubs is proposed. The concept of combining a SRLR and two loaded open stubs was employed in [8] to form a wideband BPF. In that design, a

Received 8 October 2013, Accepted 30 October 2013, Scheduled 8 November 2013

* Corresponding author: Kun Deng (dengkun139@gmail.com).

pair of perturbation stubs as long as more than half-wavelength of the square ring was installed to the ring, making up the so-called SRLR. The perturbation stubs split the degenerated modes of the ring, and the first three split resonant modes of the SRLR were utilized to design wideband BPF. The first two split modes form a dominant wideband passband, the third split mode was moved into the passband by loading two open stubs inside the ring, which achieves a sharp cut-off frequency at the right of the passband. Since the three split resonant modes are located at a lower position than the fundamental resonance of the ring, while conventional ring resonator BPFs center at the fundamental resonance of the ring, so the filter occupies the smallest circuit size in wideband ring resonator BPFs.

In this letter, a deformed structure is used to design wideband ring resonator BPF. Distinct from the layout in Ref. [8], two loaded open stubs are loaded outside the ring in this work, whereas two loaded open stubs are added inside the ring in Ref. [8]. The third split resonant mode can be moved into the dominant passband by stretching the loaded open stubs, leading to an extra bandwidth of the passband. Therefore, the proposed filter has a wider fractional bandwidth than that in Ref. [8].

2. FILTER DESIGN

The proposed filter configuration is shown in Figure 1. The proposed resonator consists of a SRLR, two square patches, and two loaded open stubs. The SRLR is formed by a square ring and a pair of bent open stubs. Two bent open stubs are used as perturbations to split the degenerated modes in the ring. The first even- and odd-

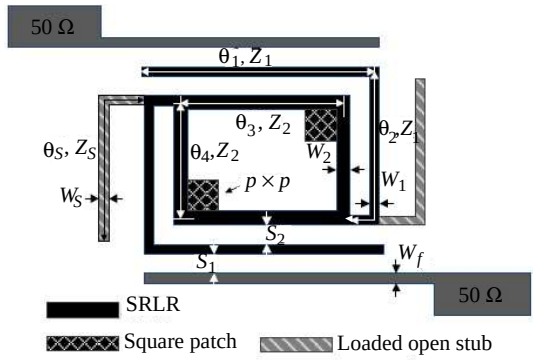

Figure 1. Layout of the proposed wideband filter.

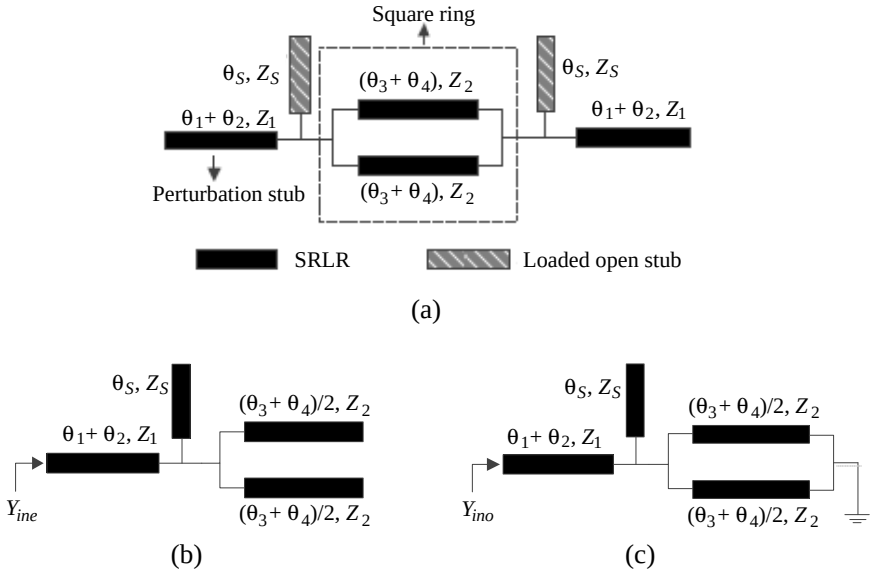

Figure 2. (a) Simplified equivalent circuit of the SRLR with two loaded open stubs. (b) Even-mode of the equivalent circuit model. (c) Odd-mode of the equivalent circuit model.

order split modes form a wideband passband under a proper external coupling, and two square patches are added in the corners of the ring to equalize the in-band ripple [8]. Two open stubs are parallel loaded with the perturbation stubs in order to control the second odd-order split mode. Even and odd analyze method is used to obtain the resonant frequencies. The resonant conditions of the SRLR can be obtained as follows [8],

$$2R_Z + \tan(\theta_1 + \theta_2) \cdot \cot\ [(\theta_3 + \theta_4)/2] = 0 \quad \text{for even mode} \quad (1)$$

$$2R_Z - \tan(\theta_1 + \theta_2) \cdot \tan\ [(\theta_3 + \theta_4)/2] = 0 \quad \text{for odd mode} \quad (2)$$

where $R_Z = Z_1/Z_2$, Z_1 and Z_2 denote the characteristic impedances of the perturbation stubs and the ring, and θ_1, θ_2 and θ_3, θ_4 indicate their electrical lengths, respectively.

With arbitrary R_Z, θ_1, θ_2, θ_3 and θ_4, resonant frequencies of all the even- and odd-order modes can be solved according to (1) and (2).

In order to have an intuitionistic understanding of the working principle of the SRLR, we fix a square ring, whose circumference is 18 mm, and then the perturbation stubs are added. Give the circumference (18 mm) of the ring, the substrate dielectric $\varepsilon_r = 2.65$, and the thickness $h = 1$ mm, the fundamental resonance of the ring

can be obtained, and the resonance is about 11.8 GHz.

Figure 3(a) plots the first three normalized resonant frequencies (f_{o1}/f_0, f_{e1}/f_0, f_{o2}/f_0) versus the normalized perturbation stub length ($k = (\theta_1 + \theta_2)/(\theta_3 + \theta_4)$), where f_0 is the fundamental resonance of the ring. From the figure, it can be found that when the perturbation stubs are stretched, f_{o1}, f_{e1}, and f_{o2} decrease fast from f_0, $2f_0$, and $3f_0$ respectively. When the normalized stub length $k > 1$, three modes are all reduced lower than f_0. Figure 3(b) depicts the simulated frequency responses of the SRLR under the conditions of no perturbation stub, weak and tight couplings with perturbation stub, where $L_i\,(i = 1, 2, 3, 4)$ is the physical length of electronic length $\theta_i\,(i = 1, 2, 3, 4)$. It can be seen that, the single ring resonator has a fundamental resonance around 11.8 GHz, which coincides with our calculated value. When the perturbation stubs are added and stretched, degenerate modes in the ring are split and the three modes (f_{o1}, f_{e1}, and f_{o2}) are shift lower simultaneously. Under a proper coupling, the first two modes (f_{o1} and f_{e1}) will form a dominant passband, while the third mode (f_{o2}) is located far away from the passband. Our next step is to move the third mode (f_{o2}) into the passband formed by f_{o1} and f_{e1}.

When two open stubs are loaded to the SRLR, the simplified equivalent circuit is shown in Figure 2(a). Its equivalent even- and odd-mode circuits are depicted in Figures 2(b) and 2(c), respectively.

For the even-order mode, the resonant condition can be derived

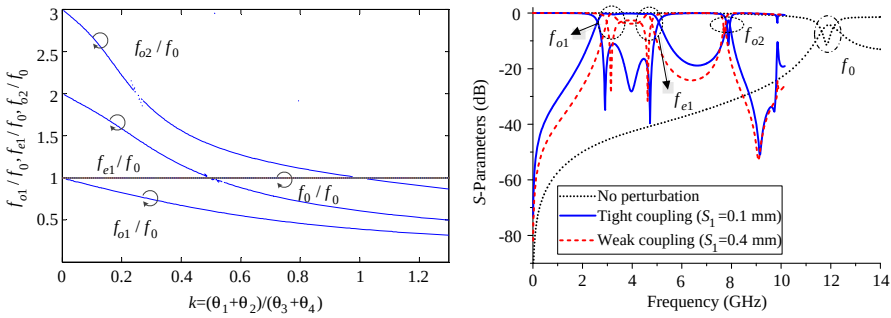

Figure 3. (a) Normalized even and odd mode resonant frequencies versus normalized perturbation stub length. (b) Simulated frequency responses of the SRLR under different conditions (Dimensions are: $L_1 = 11.5$ mm, $L_2 = 5.1$ mm, $L_3 = 4.5$ mm, $L_4 = 4.5$ mm, $S_2 = 0.2$ mm, $W_1 = 0.4$ mm, $W_2 = 0.4$ mm).

when the input admittance Y_{ine} is zero, and it is described as follows,

$$2R_Z R_S \cdot \tan[(\theta_3+\theta_4)/2] + R_Z \cdot \tan\theta_S + R_S \cdot \tan(\theta_1+\theta_2) = 0 \quad (3)$$

Similarly, the odd-order resonant condition can be obtained when the input admittance Y_{ino} is zero, and it is expressed as below,

$$R_Z \cdot \tan\theta_S \cdot \tan[(\theta_3+\theta_4)/2] - 2R_S R_Z + R_S \cdot \tan[(\theta_3+\theta_4)/2] \cdot \tan(\theta_1+\theta_2) = 0 \quad (4)$$

where $R_S = Z_S/Z_2$ and θ_S is the electrical length of the loaded open stub. When $\theta_S = 0$, resonant conditions of (3) and (4) will degenerate to (1) and (2), respectively. The loaded open-stubs will introduce a transmission zero so that the stubs can be seen as a one-quarter wavelength resonator. The resonant condition of the transmission zero can be expressed as,

$$\cot\theta_S = 0 \quad (5)$$

Figure 4(a) plots the normalized resonant frequencies of the first two odd modes, the first even mode, and the transmission zero, i.e., f_{o1}/f_0, f_{o2}/f_0, f_{e1}/f_o and f_Z/f_0 versus the length ratio of $t = \theta_S/(\theta_3+\theta_4)$ under the fixed condition of $k = 1.8$, $R_Z = 1$, and $R_S = 1$. Where f_0 is the fundamental resonance of the ring resonator, and $k = (\theta_1+\theta_2)/(\theta_3+\theta_4)$. It can be seen that, as t increases from 0.5 to 1.5, the second odd-order mode f_{o2} decreases fast while the first odd-order mode f_{o1} and the first even-order mode f_{e1} keep almost constant. The transmission zero frequency f_Z decreases fast simultaneously with the second odd-order mode f_{o2}, but it is always located at a higher frequency than f_{o2}. Figure 4(b) shows the simulated frequency responses of the three resonances (f_{o1}, f_{e1}, and f_{o2}) and the

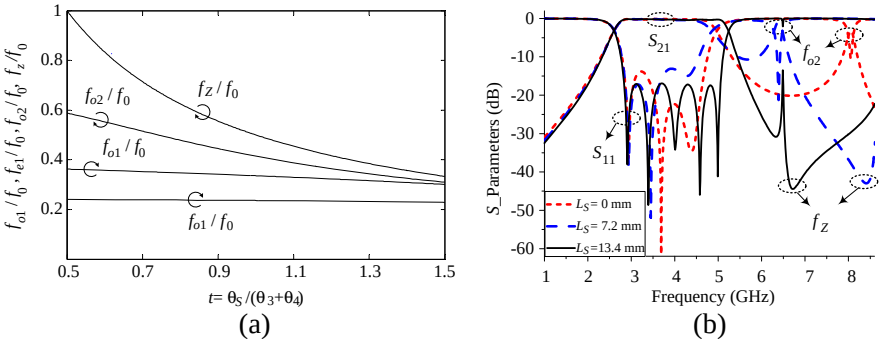

Figure 4. (a) Normalized resonant frequencies of the SRLR with loaded open-stubs. (b) Simulated frequency responses against different loaded stub length ($L_1 = 11.5$ mm, $L_2 = 5.1$ mm, $L_3 = 4.5$ mm, $L_4 = 4.5$ mm, $S_1 = 0.1$ mm, $S_2 = 0.2$ mm, $W_1 = 0.4$ mm, $W_2 = 0.4$ mm).

transmission zero frequency (f_Z) against different length (L_S, physical length of θ_S) of the loaded open-stub. It can be found that when the loaded stubs are stretched, the dominant passband has little change, the second odd-order resonance (f_{o2}) is moved into the passband, and a transmission zero is brought in at the right of the passband. Finally, the initial dominant passband is extended by the second odd-order mode (f_{o2}).

The design procedures of the proposed wideband filter can be summarized as follows [8]. First, determine the dimensions of the SRLR and the loaded open stubs to meet the respective band frequencies and the required bandwidths. Second, determine the feed circuit dimensions to satisfy the external quality factor. Then add two square patches to smooth the passband ripple. Finally, the optimized wideband performance can be obtained.

It should be noted that in this design, the length ratio of the perturbation stub to the circumference of square ring, i.e., $k = (\theta_1 + \theta_2)/(\theta_3 + \theta_4)$, should be select in the experiential range of [1.4, 2], distinct from [1.2, 1.4] in Ref. [8]. The reason is that a wider fractional bandwidth needs a longer parallel-coupled microstrip line (PCML) to provide proper external coupling in case of the same line widths.

Additionally, cross coupling between the strips of the proposed resonator may be considered confusing. In fact, the coupling only changes the impedances of the perturbation stub and the ring. In order to facilitate the analysis, the cross coupling was ignored. Actually, the impedance variation caused by the cross coupling have a slight effect on the performance of the filter, and the changes can be calibrated by adjusting the line widths of the perturbation stub or the ring so as to obtain an accurate impedance. For demonstration, a SRLR with fixed perturbation stub and perimeter of the ring is analyzed.

By keeping the following dimensions unchanged, $L_1 + L_2 = 11.5 + 5.1 = 16.6\,\text{mm}$, $L_3 = 4.5\,\text{mm}$, $L_4 = 4.5\,\text{mm}$, $W_1 = 0.4\,\text{mm}$, $W_2 = 0.4\,\text{mm}$, frequency responses of the SRLR with different gap width S_2 under weak coupling ($S_1 = 0.6\,\text{mm}$) are compared. Figure 5(a) shows the simulated results of the SRLR with the dimensions mentioned above, it can be found that under a tight crossing coupling ($S_2 = 0.2\,\text{mm}$) the first two modes (f_{o1} and f_{e1}) locate at 3.21 and 4.59 GHz, respectively. When the gap width S_2 increases to 3 mm, the cross coupling is very slight and can be ignored. The first two modes (f_{o1} and f_{e1}) shift to 2.77 and 4.7 GHz, respectively. Compared with the tight cross coupling, the two modes under the weak cross coupling depart from each other, and the separation increases about 0.55 GHz. No matter under weak or tight cross coupling, the frequency responses seem to be the same. Meanwhile, the frequency separation

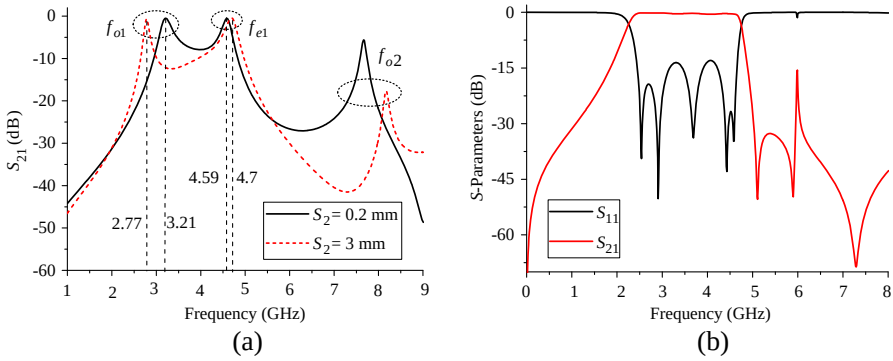

Figure 5. (a) Simulated frequency responses of the SRLR versus different gap width S_2 under weak coupling. (b) Simulated frequency responses of the resonator in Figure 1 with a wide gap S_2, dimensions are: $L_1 = 6$, $L_2 = 11.25$, $L_3 = 4.5$, $L_4 = 4.5$, $L_S = 10.8$, $W_1 = 0.3$, $W_2 = 0.4$, $W_S = 0.4$, $W_f = 0.4$, $S_1 = 0.1$, $S_2 = 3$, $p = 2$, in mm.

$f_{e1} - f_{o1}$ is controlled by the line widths of W_1 and W_2 [8, 15], so the frequency separation can be calibrated by changing the line widths of the perturbation and the ring if the gap S_2 is changed. Therefore, we can conclude that the cross coupling has little effect on the filter performance and can be omitted during our design procedure. Figure 5(b) describes the simulated frequency responses of the resonator in Figure 1 with $S_2 = 3$ mm, and we can find that under a weak cross coupling the resonator still can be used for wideband operation, thus the cross coupling can be ignored during our design procedure.

3. MEASUREMENT RESULT

A substrate with a relative dielectric of $\varepsilon_r = 2.65$ and thickness of $h = 1$ mm is chosen for implementation of the proposed filter. A commercial full-wave simulator, IE3D, is utilized for further analysis and optimization. Figure 6(a) depicts the photograph of the fabricated filter. Its optimized dimensions are: $L_1 = 11.5$ mm, $L_2 = 5.1$ mm, $L_3 = 4.5$ mm, $L_4 = 4.5$ mm, $L_S = 13.4$ mm, $S_1 = 0.1$ mm, $S_2 = 0.2$ mm, $W_1 = 0.4$ mm, $W_2 = 0.4$ mm, $W_S = 0.4$ mm, $W_f = 0.4$ mm, $p = 1$ mm. The overall size is 19.5×7.1 mm^2, approximately $0.34\lambda_g \times 0.12\lambda_g$, where λ_g is the wave-guided length of the filter at center frequency. The measured and simulated results are indicated in Figure 6(b). The measured results show that the center frequency of the filter

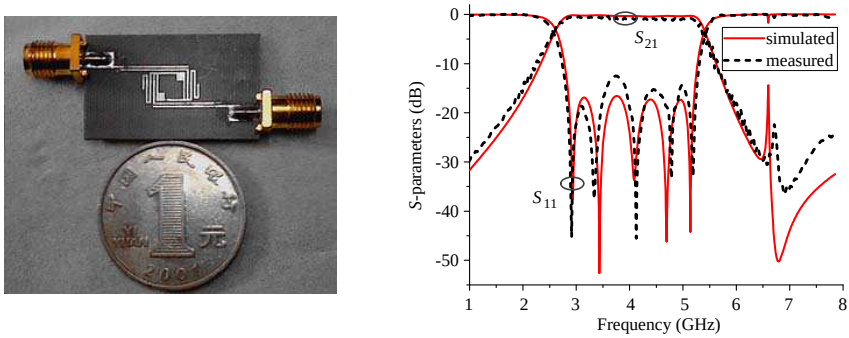

Figure 6. (a) Photograph of the fabricated filter. (b) Comparison of the simulated and measured results of frequency responses.

Table 1. Comparison of the wideband microstrip ring resonator BPFs.

Wideband BPF	Substrate	Center frequency (GHz)	FBW (3 dB)	Size ($\lambda_g \times \lambda_g$)
Figure 9(b) in Ref. [9]	$\varepsilon_r = 10.8$, $h = 0.635$ mm	4.2	64%	0.41×0.41
Figure 7 in Ref. [10]	$\varepsilon_r = 3.2$, $h = 0.762$ mm	5	52%	0.85×0.85
Figure 5 in Ref. [11]	$\varepsilon_r = 6.15$, $h = 0.635$ mm	2.5	87.3%	0.73×0.4
Figure 1 in Ref. [12]	$\varepsilon_r = 11.2$, $h = 1.6$ mm	1.45	57.9%	0.77×0.13
Figure 1 in Ref. [13]	$\varepsilon_r = 9.8$, $h = 1.27$ mm	2	30%	0.27×0.27
Figure 8 in Ref. [14]	$\varepsilon_r = 4.55$, $h = 0.8$ mm	1.02	29.36%	0.41×0.48
Figure 6(a) in Ref. [8]	$\varepsilon_r = 2.65$, $h = 1$ mm	3.5	56.5%	0.18×0.1
Figure 6(a) in this work	$\varepsilon_r = 2.65$, $h = 1$ mm	3.98	69.2%	0.34×0.12

is 3.98 GHz, and that its 3 dB fractional bandwidth is 69.2%. The measured minimum insertion loss is about 0.9 dB and the return loss is around 15 dB.

Table 1 compares the circuit size of the filter in this paper with the previous work [8] and those conventional ring resonator wideband

BPFs in [9–13]. λ_g is the wave-guided length at center frequency. It can be found that, the proposed filter has a relatively larger circuit size than the previous work [8] does. The reason is that the perturbation stubs in this work is longer than those in the previous work. However, the circuit size of the proposed filter is still smaller than those of the conventional ring resonator BPFs [9–14].

4. CONCLUSION

A wideband microstrip bandpass filter based on square ring loaded resonator has been proposed in this paper. Without introducing any additional resonators or filtering components, an extra fractional bandwidth is achieved by the deformed new structure, compared with the previous work [8]. The measured and simulated results agree well with each other, which validates the application feasibility of the proposed filter.

ACKNOWLEDGMENT

This work was supported by the National High Technology Research and Development Program of China (863 Program) No. 2012AA01A308 and the National Natural Science Foundation of China (NSFC) under Project Nos. 61271017 and 61072017.

REFERENCES

1. Ren, S.-W., H.-L. Peng, J.-F. Mao, and A. M. Gao, "Compact quasi-elliptic wideband bandpass filter using cross-coupled multi-mode resonator," *IEEE Microw. Wireless Compon. Lett.*, Vol. 22, No. 8, 397–399, Aug. 2012.
2. Sohail, K., P.-W. Wong, and Y.-C. Lee, "Synthesis and design of four pole ultra-wide band (UWB) bandpass filter (BPF) employing multi-mode resonators (MMR)," *IEEE MTT-S Int. Microw. Symp. Dig.*, 1–3, Jun. 2012.
3. Chen, C.-P., J. Oda, T. Anada, Z. Ma, and S. Takeda, "Theoretical design of wideband filters with attenuation poles using improved parallel-coupled three-line units," *IEEE MTT-S Int. Microw. Symp. Dig.*, 1–3, Jun. 2012.
4. Amir, N., M. Masoud, and H. Ahmad, "A novel wideband stepped-impedance rectangular-ring resonator bandpass filter with two notched bands," *IEEE MTT-S Int. Microw. Symp. Dig.*, 1–3, Jun. 2012.

5. Chen, D., L. Zhu, and C.-H. Cheng, "A novel wideband bandpass filter using stub-loaded ring resonator and tapped feed," *Progress In Electromagnetics Research Letters*, Vol. 42, 37–44, 2013.
6. Cao, H.-L., S.-J. He, H. Li, and S.-Z. Yang, "A compact wideband bandpass filter using novel CSRR loaded QMSIW resonator with high selectivity," *Progress In Electromagnetics Research C*, Vol. 41, 239–254, 2013.
7. Wei, F., Z.-D. Wand, F. Yang, and X.-W. Shi, "Compact UWB BPF with triple-notched bands based on stub loaded resonator," *Electron. Lett.*, Vol. 49, No. 2, 124–126, Jan. 2013.
8. Deng, K., J.-Z. Chen, B. Wu, T. Su, and C.-H. Liang, "Miniaturized wideband bandpass filter utilizing square ring resonator and loaded open-stub," *Progress In Electromagnetics Research C*, Vol. 39, 179–192, 2013.
9. Sun, S. and L. Zhu, "Wideband microstrip ring resonator bandpass filters under multiple resonances," *IEEE Trans. Microw. Theory Tech.*, Vol. 55, No. 10, 2176–2182, Oct. 2007.
10. Ahonnom, S. and P. Akkaraekthalin, "Wideband dual mode microstrip bandpass filters using a new perturbation with notch rectangular slots," *Proceeding of ECTI-CON*, Vol. 1, 269–272, 2008.
11. Kim, C.-H. and K. Chang, "Wideband ring resonator bandpass filter with dual stepped impedance stubs," *IEEE MTT-S Int. Microw. Symp. Dig.*, 229–232, May 2010.
12. Fan, J., D.-Z. Zhan, C.-J. Jin, and J.-R. Luo, "Wideband microstrip bandpass filter based on quadruple mode ring resonator," *IEEE Microw. Wireless Compon. Lett.*, Vol. 22, No. 7, 348–350, Jul. 2012.
13. Ma, Z.-W., H. Sasaki, C.-P. Chen, T. Anada, and Y. Kobayashi, "Design of a wideband bandpass filter using microstrip parallel-coupled dual-mode ring resonator," *Asia-Pacific Microwave Conference Proceedings*, 21–24, Dec. 2010.
14. Srisathit, K., A. Worapishet, and W. Surakampontorn, "Design of tripple-mode ring resonator for wideband microstrip bandpass filters," *IEEE Trans. Microw. Theory Tech.*, Vol. 58, No. 11, 2867–2877, Nov. 2010.
15. Deng, K., S. Yang, S.-J. Sun, B. Wu, and X.-W. Shi, "Dual-mode dual-band bandpass filter based on square loop resonator," *Progress In Electromagnetics Research C*, Vol. 37, 119–130, 2013.